ANTAGONISM OF THE PROINFLAMMATORY AND PRONOCICEPTIVE ACTIONS OF CANONICAL AND BIASED AGONISTS OF PROTEASE-ACTIVATED RECEPTOR-2

T Lieu[1,2], P Zhao[1,2], E Savage[1,2], L Edgington-Mitchel[1,2],

R Bron[1,2], D P Poole[1,2,3], R-J Lohman[4], D Fairlie[4], N W Bunnett[1,2,5]

[1]Monash Institute of Pharmaceutical Sciences and [2]Australian Research Council Centre of Excellence in Convergent Bio-Nano Science and Technology, Monash University, Parkville, Australia; Department of [3]Anatomy and Neuroscience, and [5]Pharmacology and Therapeutics, University of Melbourne, Melbourne, Australia; [4]Institute of Molecular Biosciences, University of Queensland, Brisbane, Australia.

To whom correspondence should be addressed: Nigel Bunnett, Ph.D., Monash Institute of Pharmaceutical Sciences, 381 Royal Parade, Parkville, VIC 3052, Australia. Tel: Office - +61 3 9903 9136; Mobile - +61 407 392 619. Facsimile: +61 3 9903 9581. Email: Nigel.Bunnett@Monash.edu

Running Title: Antagonism of canonical and biased PAR_2 agonists

ABSTRACT

Background and Purpose. Diverse proteases cleave protease-activated receptor 2 (PAR_2) on primary sensory neurons and epithelial cells to evoke pain and inflammation. Trypsin and tryptase activate PAR_2 by a canonical mechanism that entails cleavage within the extracellular N-terminus revealing a tethered ligand that activates the cleaved receptor. Cathepsin-S and elastase are biased agonists that cleave PAR_2 at distinct sites to initiate different signaling pathways. Although PAR_2 is a therapeutic target for inflammatory and painful diseases, the divergent mechanisms of proteolytic activation complicate the development of therapeutically useful antagonists.

Experimental Approach. We investigated whether the PAR_2 antagonist N-[(2S)-3-cyclohexyl-1-[[(2S,3R)-3-methyl-1-oxo-1-spiro[indene-1,4'-piperidine]-1'-ylpentan-2-yl]amino]-1-oxopropan-2-yl]-1,2-oxazole-5-carboxamide (GB88) inhibits protease-evoked activation of nociceptors and protease-stimulated oedema and hyperalgesia in rats and mice.

Key Results. Intraplantar injection of trypsin, cathepsin-S and elastase stimulated mechanical and thermal hyperalgesia and oedema in mice. Oral GB88 or *Par2* deletion inhibited the algesic and proinflammatory actions of canonical and biased proteases, but did not affect basal responses. GB88 prevented pronociceptive and proinflammatory effects of the PAR_2-selective agonists 2-furoyl-LIGRLO-NH_2 and AC264613. GB88 did not affect capsaicin-evoked hyperalgesia or inflammation. Trypsin, cathepsin-S and elastase increased $[Ca^{2+}]_i$ in rat nociceptors, which expressed PAR_2. GB88 inhibited activation of nociceptors by canonical and biased proteases, but did not affect capsaicin-evoked activation of nociceptors. GB88 did not affect trypsin or elastase activities, and inhibited cathepsin-S activity only at high concentrations.

Conclusions and Implications. GB88 inhibits the capacity of canonical and biased proteases to activate nociceptors and cause pain and inflammation.

INTRODUCTION

Serine, cysteine and metallo-proteases can signal to cells by cleaving protease-activated receptors (PARs), a family of four G-protein coupled receptors (PAR_{1-4}) (Hollenberg *et al.*, 2014; Ossovskaya *et al.*, 2004; Zhao *et al.*, 2014b). PAR_2 is expressed by epithelial, endothelial and smooth muscle cells, as well as by cells of the immune and nervous systems (Bohm *et al.*, 1996; Nystedt *et al.*, 1995; Nystedt *et al.*, 1994). Proteases that activate PAR_2 in primary sensory neurons stimulate the release of substance P and calcitonin-gene-related peptide in peripheral tissues, leading to neurogenic inflammation (Steinhoff *et al.*, 2000). PAR_2 can also sensitize and activate transient receptor potential (TRP) ion channels in primary sensory neurons, including TRP vanilloid 1 and 4 (TRPV1, TRPV4) and ankyrin 1 (TRPA1) (Amadesi *et al.*, 2006; Amadesi *et al.*, 2004; Dai *et al.*, 2004; Dai *et al.*, 2007; Grant *et al.*, 2007; Poole *et al.*, 2013), which results in central transmission, neuropeptide release in the spinal cord, and pain transmission (Vergnolle *et al.*, 2001). Proteases that activate PAR_2 on epithelial cells can promote disassembly of tight junctions (Jacob *et al.*, 2005), induce cyclooxygenase 2 (Wang *et al.*, 2008), and stimulate release of proinflammatory cytokines (Wang *et al.*, 2010). PAR_2 deletion abrogates inflammatory and painful disorders of the airways, joints, colon and skin (Cattaruzza *et al.*, 2011; Cottrell *et al.*, 2007; Ferrell *et al.*, 2003; Lindner *et al.*, 2000; Schmidlin *et al.*, 2002; Shichijo *et al.*, 2006). These observations suggest that PAR_2 is an important target for inflammatory and painful disorders. However, the development of therapeutically useful antagonists is hampered by the unusual mechanism of PAR_2 activation.

The canonical mechanism by which trypsin and tryptase activate PAR_2 involves hydrolysis of $Arg^{36}{\downarrow}Ser^{37}$ and exposure of the tethered ligand S^{37}LIGKV (human PAR_2), which binds to and activate the cleaved receptor (Bohm *et al.*, 1996; Corvera *et al.*, 1997; Nystedt *et al.*, 1994). Synthetic peptides that mimic the tethered ligand can directly activate PAR_2 and are useful tools to probe receptor function. Trypsin-activated PAR_2 couples to Gαq and phospholipase Cβ, leading to mobilization of intracellular calcium and activation of protein kinases (PK) C and D ((Amadesi *et al.*, 2006; Amadesi *et al.*, 2009). Trypsin-activated

PAR_2 also recruits G protein receptor kinase 2 and β-arrestins, which mediate PAR_2 endocytosis and ERK1/2 signaling from endosomes (Ayoub *et al.*, 2013; DeFea *et al.*, 2000; Dery *et al.*, 1999; Jensen *et al.*, 2013). The development of PAR_2 antagonists is complicated by this mechanism of intramolecular receptor activation by a proteolytically-exposed tethered ligand. Another complication is the existence of divergent mechanisms of proteolytic activation (Hollenberg *et al.*, 2014; Zhao *et al.*, 2014b). Proteases that cleave PAR_2 distal to the canonical cleavage site can disarm the receptor by removing the trypsin-exposed tethered ligand. Thus, neutrophil/leukocyte elastase cleaves PAR_2 at $Ser^{67}\downarrow Val^{68}$, which removes the trypsin cleavage site and thereby blocks the ability for trypsin to activate the receptor (Dulon *et al.*, 2003; Ramachandran *et al.*, 2011). However, proteases that cleave PAR_2 at distinct sites within the N-terminal domain can reveal different tethered ligands or stabilize unique receptor conformations, and can thereby act as biased agonists that promote PAR_2 coupling to divergent signaling pathways. Cathepsin-S (Cat-S), a cysteine protease secreted by antigen-presenting cells, cleaves PAR_2 at $Glu^{56}\downarrow Thr^{57}$, to reveal a distinct tethered ligand that promotes PAR_2 coupling to Gαs, adenylyl cyclase, cAMP and PKA, but not to Gαq and β-arrestins (Zhao *et al.*, 2014a). Cat-S can also cleave PAR_2 at $Gly^{41}\downarrow Lys^{42}$ (Elmariah *et al.*, 2014). Elastase is also a biased agonist that promotes PAR_2 coupling to Gαs, adenylyl cyclase, cAMP and PKA, but not to Gαq and β-arrestins, although elastase does not activate PAR_2 by a tethered ligand mechanism (Ramachandran *et al.*, 2011; Zhao *et al.*, 2015). Despite these divergent mechanisms of PAR_2 activation, canonical and biased proteases cause PAR_2- and TRPV4-dependent inflammation and pain (Grant *et al.*, 2007; Poole *et al.*, 2013; Zhao *et al.*, 2014a; Zhao *et al.*, 2015). Thus, a requirement of therapeutically useful antagonists is that they disrupt the capacity of diverse proteases to activate PAR_2 by canonical and biased mechanisms.

Although antibodies that target the canonical PAR_2 cleavage site have efficacy in preclinical models of inflammatory disease (Kelso *et al.*, 2006), it is uncertain whether they can block activation of the receptor by biased proteases that cleave at distant sites. The small molecule PAR_2 antagonist ENMD-1068 and peptidomimetic antagonists based on the

canonical tethered ligand domain, including K-14585 and C391, can also inhibit PAR_2-mediated inflammation and pain, but their ability to suppress biased mechanisms of PAR_2 activation has not been explored (Boitano *et al.*, 2015; Goh *et al.*, 2009; Kelso *et al.*, 2006). GB83 and GB88 are small molecules that can inhibit PAR_2 activation by trypsin and tethered ligand-derived agonists, and are efficacious in preclinical models of inflammatory disease (Barry *et al.*, 2010; Lohman *et al.*, 2012a; Lohman *et al.*, 2012b; Suen *et al.*, 2012). However, it is not known whether GB88 can antagonize the actions of canonical and biased agonists of PAR_2 on nociceptor activity and nociception. We examined the effects of GB88 on the capacity of canonical and biased proteases to activate nociceptors and induce pain and inflammation.

METHODS

Materials. GB88 (N-[(2S)-3-cyclohexyl-1-[[(2S,3R)-3-methyl-1-oxo-1-spiro[indene-1,4'-piperidine]-1'-ylpentan-2-yl]amino]-1-oxopropan-2-yl]-1,2-oxazole-5-carboxamide) was prepared as described (Barry *et al.*, 2010; Suen *et al.*, 2012). The PAR_2 agonists 2-furoyl-LIGRLO-NH_2 was from American Peptide Company Inc. (Sunnyvale, CA) and AC264613 was from Tocris Biosciences (Bristol, UK). Human pancreatic trypsin (100,000 U/ml) was from Sigma-Aldrich (St. Louis, MO). Human Cat-S (0.4 U/ml) was a gift from Medivir AB (Huddinge, Sweden) and has been described (Zhao *et al.*, 2014a). Human sputum elastase (864 U/mg) was from Elastin Products Company (Owensville, MO). Fluorogenic protease substrates were from Bachem AG (Budendorf, Switzerland): trypsin, H-D-Ala-Leu-Lys-AMC; elastase, MeOSuc-Ala-Ala-Pro-Val-AMC; Cat-S, Bock-Val-Leu-Lys-AMC. The activity-based protease probes Cy5-ProLys-diphenyl phosphonate (PK-DPP), Cy5-Val-diphenyl phosphonate (V-DPP) and BMV109 were synthesized as described (Gilmore *et al.*, 2009; Pan *et al.*, 2006; Verdoes *et al.*, 2013). Unless otherwise indicated, other reagents were from Sigma-Aldrich (St. Louis, MO).

Animals. The Animal Ethics Committee of Monash University approved procedures using animals. Male C57BL/6, *Par2-/-* and *Par2+/+* littermates (Lindner *et al.*, 2000) (8-12 weeks),

and male Sprague-Dawley rats (7-8 weeks) were studied. Animals were maintained under temperature (22±4°C) and light- (12 h light/dark cycle) controlled conditions with free access to food and water.

Mechanical hyperalgesia and oedema. Mice were placed in individual cylinders on a mesh stand. They were acclimatized to the experimental room, restraint apparatus, and investigator for 2 h periods on 2 successive days before experiments. To assess mechanical pain, paw withdrawal in response to stimulation of the plantar surface of the hind paw with graded von Frey filaments (0.078, 0.196, 0.392, 0.686, 1.569, 3.922, 5.882, 9.804, 13.725, and 19.608 mN) was determined using the "up-and-down" paradigm (Alemi *et al.*, 2013; Chaplan *et al.*, 1994). In this analysis, an increase in the filament stiffness required to induce paw withdrawal indicates mechanical analgesia, whereas a decrease in the filament stiffness required to induce withdrawal indicates mechanical hyperalgesia. On the day before the study, von Frey scores were measured in triplicate to establish a baseline for each animal. To assess inflammatory oedema of the paw, hind paw thickness was measured using digital callipers before and after treatments (Alemi *et al.*, 2013).

Thermal hyperalgesia. For studies of thermal hyperalgesia, paw withdrawal latencies to thermal stimulation of one hind paw was measured in unrestrained mice using Hargreaves's apparatus (Amadesi *et al.*, 2004; Hargreaves *et al.*, 1988). An increase in latency indicates thermal analgesia, whereas a decrease in latency indicates thermal hyperalgesia. Mice were acclimatized to the Hargreaves' apparatus for 1 h, and then baseline readings were collected.

PAR_2 antagonist and agonists. Investigators were blinded to the experimental treatments. GB88 (10 mg/kg) or vehicle (control, 0.9% NaCl) was administered by gavage (150 µl) 2 h before intraplantar injections. For intraplantar injections, mice were sedated with 5% isoflurane. Trypsin (140 nM, 0.04 U/µl), elastase (1.18 µM, 0.03 U/µl), Cat-S (2.5 µM, 0.06 U/µl), 2-furoyl-LIGRLO-NH_2 (64 µM, 50 ng/µl), AC264613 (250 µM, 100 ng/µl), capsaicin (1.6 µM, 0.5 ng/µl) or vehicle (0.9% NaCl) was injected subcutaneously into the plantar surface of the left hind paw (10 µl). Mechanical hyperalgesia, paw thickness and thermal hyperalgesia were measured hourly for 4 h.

***In situ* hybridization.** cDNAs for mouse and rat PAR_2 were amplified by RT-PCR using RNA from mouse or rat colon. The following forward and reverse primers were used: mouse PAR_2, CACCGGGACGCAACAACAGTAAAG (mPar2_F199) and GAATTCTAATACGACTCACTAT AGGGAGATATGCAGCTGTTGAGGGTCGACAG (mPar2_R1136_T7); rat PAR_2, GAATGCACCGGGACCCAACAGTAA (rPAR2_F165) and GAATTCTAATACGACTCACTAT AGGGAGATGGAGGTGAGCGATATCTGCATGC (rPAR2_R1216_T7). The design of the reverse primers included the T7 promoter sequence (underlined), which allowed the PCR products to be used directly for the generation of digoxigenin (DIG)-labelled antisense cRNA probes by *in vitro* transcription with T7 RNA polymerase (Roche Products, Dee Why, NSW). Sections (12 µm) of mouse and rat dorsal root ganglia (DRG) or trigeminal ganglia (levels) were processed for combined *in situ* hybridisation and immunofluorescence as described (Bron *et al.*, 2014; Lieu *et al.*, 2014). The following primary antibodies were used: rabbit anti-CGRP (Sigma #C8198; 1:2,000), mouse anti-heavy chain neurofilament (NF200, Sigma; #N0142; 1,000). Biotinylated isolectin B4 (IB4) was from Sigma (#L2140). Secondary antibodies used were donkey ant-mouse-Alexa-488 (1:500), donkey anti-rabbit-Alexa568 (1:1,000) and streptavidin-Alexa647 (1:500) (Thermofisher Scientific, Carlsbad, CA). Sections were examined and photographed using 10x or 20x objective magnification on a Zeiss Axioskope.Z1 fluorescence microscope (Zeiss, Oberkocken, Germany). Digitized images were processed using the Zeiss Zen software and exported as TIFF files to Adobe Photoshop for figure preparation.

Dissociation of DRG neurons. DRG neurons were collected from Sprague Dawley rats. Neurons were dispersed as described with modifications (Zhao *et al.*, 2014a; Zhao *et al.*, 2015). Briefly, DRG from all levels were incubated with collagenase IV (2 mg/ml), dispase II (2 mg/ml) and DNase I (100 µg/ml) for 40 min at 37°C. Cells were centrifuged (5 min, 500 g), re-suspended in Hanks Balanced Salt Solution (HBSS), and filtered through a 40 µm nylon mesh. Filtered cells were centrifuged, re-suspended in 1 ml of HBSS, and layered onto a 20% Percoll solution comprising 1 ml Percoll and 4 ml L-15 (Lebovitz) medium

(ThermoFisher Scientific). The gradient was centrifuged (9 min, 800 g). The supernatant was removed and the cell pellet was washed with 10 ml of L-15. Neurons were plated onto 96 well plates coated with laminin (0.004 mg/ml) and poly-D-lysine (0.1 mg/ml). Neurons were cultured in L-15 Lebovitz medium containing 10% foetal calf serum, with penicillin and streptomycin and maintained at 37ºC for 16 h.

Measurement of $[Ca^{2+}]_i$ in DRG neurons. Neurons were loaded with Fura-2/AM (2 μM) for 1.5 h at 37°C. Neurons were mounted in microincubator in calcium buffer (150 mM NaCl, 2.6 mM KCl, 0.1 mM $CaCl_2$, 1.18 mM $MgCl_2$, 10 mM D-glucose, 10 mM HEPES, pH 7.4) at 37°C on the stage of a Leica DMI6000B microscope equipped with a PL APO ×20 NA0.75 objective (Leica Microsystems, North Ryde, NSW). Fluorescence was measured at 340 and 380 nm excitation with 530 nm emission using an Andor iXon 887 camera (Andor Technology, Belfast) and MetaFluor version 7.8.0 software (Molecular Devices, Sunnyvale, CA). Neurons were challenged sequentially with trypsin (10 nM, 2.85 mU/ μl), elastase (100 nM, 2.54 mU/μl), or Cat-S (100 nM, 2.4 mU/μl), followed by capsaicin (1 μM) and KCl (50 mM). In some experiments, neurons were pre-treated with GB88 (10 μM) or vehicle (control) for 30 min before stimulation with proteases. Images were analysed using a custom journal in MetaMorph software version 7.8.2. A maximum intensity image was generated and projected through time to generate an image of all cells. Cells were segmented and binarised from this image using the Multi Wavelength Cell Scoring module on the basis of size and fluorescence intensity. Neurons of interest (<25 μm diameter) were selected. Results are expressed as the proportion of capsaicin- and KCl-responsive neurons that also responded to proteases.

Fluorogenic protease assays. GB88 (10 μM) was pre-incubated with the appropriate fluorogenic substrate (50 μM): trypsin, H-D-Ala-Leu-Lys-AMC; elastase, MeOSuc-Ala-Ala-Pro-Val-AMC, Cat-S: Bock-Val-Leu-Lys-AMC. Proteases were added to give final concentrations of 10 nM trypsin, 100 nM elastase, or 100 nM Cat-S. Substrate cleavage was assessed by measuring fluorescence during the initial 60-120 s (ex/em 360/440 nm). The slope was determined in the linear range and presented as a percentage of the control.

Covalent activity-based probe protease assays. Recombinant proteases (100 ng) were diluted in 20 µl PBS containing GB88 (0, 1, 10 or 100 µM) and DMSO (1%), and were incubated for 30 min at 37°C. The appropriate activity-based probes were added: trypsin, PK-DPP (1 µM); elastase, V-DPP (1 µM), Cat-S, BMV109 (100 nM) (Gilmore *et al.*, 2009; Pan *et al.*, 2006; Verdoes *et al.*, 2013). Proteases were incubated with activity-based probes for 5 min at 37°C, solubilized with sample buffer, boiled, and separated on a 15% SDS-PAGE gel. Probe labelling was detected by scanning gels for Cy5 fluorescence using a Typhoon FLA 7000 Scanner (GE Healthcare, Parramatta, NSW).

Statistical Analyses. Results are expressed as mean ± SEM. Data were analysed in GraphPad Prism 6.0using Student's *t*-test or ANOVA followed by Dunnett's *post hoc* test. Differences between means with a *P*-value <0.05 were considered significant.

RESULTS

GB88 antagonism of the proinflammatory and pronociceptive actions of canonical and biased protease agonists of PAR_2. Proteases that cleave PAR_2 at different sites within the extracellular N-terminal domain can activate canonical or biased pathways of signaling (Hollenberg *et al.*, 2014; Ramachandran *et al.*, 2011; Zhao *et al.*, 2014a; Zhao *et al.*, 2015; Zhao *et al.*, 2014b). Although PAR_2 deletion attenuates the pronociceptive and proinflammatory actions of trypsin, tryptase, elastase and Cat-S (Vergnolle *et al.*, 2001; Zhao *et al.*, 2014a; Zhao *et al.*, 2015), a pharmacological inhibitor pain and inflammation evoked by biased proteases has not been identified. We evaluated whether GB88 inhibits trypsin-, elastase- and Cat-S-evoked pain and inflammation in mice.

Intraplantar injection of trypsin stimulated an 11.5 ± 1.8% increase in paw thickness within 1 h that was sustained for 4 h, indicative of oedema (Fig. 1A). Trypsin reduced the von Frey response from 2-4 h, consistent with mechanical hyperalgesia (Fig. 1B), and decreased the latency of paw withdrawal to heat from 3-4 h, indicating thermal hyperalgesia (Fig. 1C). Oral administration of GB88 2 h before injection of trypsin reduced the effects of trypsin on

paw thickness by ~50%, and prevented trypsin-evoked mechanical and thermal hyperalgesia (Fig. 1 A-C).

Intraplantar Cat-S caused a 16.3 ± 3.9% increase in paw thickness within 1 h, which was sustained for 4 h (Fig. 1D). Cat-S reduced the von Frey response from 1-4 h (Fig. 1E), and decreased latency time to paw withdrawal from heat at 2-4 h (Fig. 1F). GB88 abolished-Cat-S evoked oedema, and attenuated Cat-S-stimulated mechanical and thermal hyperalgesia (Fig. 1 D-F).

Intraplantar elastase caused a 9.49 ± 2.8 % increase of paw thickness at 1 h that was sustained for 4 h (Fig. 1G). Elastase reduced the von Frey response from 2-3 h, consistent with mechanical hyperalgesia (Fig. 1H). In contrast to trypsin and Cat-S, elastase did not evoke thermal hyperalgesia (Fig. 1I). GB88 attenuated elastase-induced oedema and mechanical hyperalgesia (Fig. 1 G-I).

Intraplantar injection of vehicle did not induce oedema or mechanical hypersensitivity, and GB88 did not affect baseline paw thickness (Fig. 2 A) or mechanical sensitivity (Fig. 2 B).

Thus, GB88 inhibits the proinflammatory and pronociceptive actions of proteases that activate PAR_2 by canonical and biased mechanisms.

GB88 antagonism of the proinflammatory and pronociceptive actions of PAR_2 agonists. Synthetic peptides that mimic the trypsin-exposed tethered ligand can directly activate PAR_2. Like trypsin, these activating peptides induce PAR_2 coupling to Gαq and β-arrestins, sensitize TRP channels, and cause inflammation and pain (Amadesi *et al.*, 2006; Dai *et al.*, 2007; Grant *et al.*, 2007; Poole *et al.*, 2013; Steinhoff *et al.*, 2000; Vergnolle *et al.*, 2001). We investigated whether GB88 inhibits the proinflammatory and algesic actions of 2-furoyl-LIGRLO-NH_2, an analogue of the tethered ligand domain (Kanke *et al.*, 2005), and AC264613, a small molecule agonist of PAR_2 that elicits thermal hyperalgesia and oedema (Gardell *et al.*, 2008).

Intraplantar injection of 2-furoyl-LIGRLO-NH_2 caused a 20.7 ± 2.8% paw thickness at the 1 h, which was sustained for 4 h (Fig. 3A). 2-furoyl-LIGRLO-NH_2 reduced the von Frey withdrawal response from 2-4 h, indicative of mechanical hyperalgesia (Fig. 3B). GB88

abolished 2-furoyl-LIGRLO-NH_2-evoked oedema and reduced mechanical hyperalgesia by 30% (Fig. 3A, B).

Intraplantar injection of AC264613 induced a 10.3 ± 1.9 % increase in paw thickness at 1 h that was persistent for 4 h (Fig. 3C). AC264613-evoked robust mechanical hyperalgesia at 1 h that was persistent for 4 h (Fig. 3D). GB88 prevented AC264613-stimulated inflammation and pain (Fig. 3C, D).

Thus, GB88 inhibits the effects of small molecule synthetic agonists of PAR_2 on inflammation and pain.

Effects of GB88 on capsaicin-evoked inflammation and pain. The capacity of GB88 to inhibit protease- and PAR_2-evoked inflammation and nociception could be due to antagonism of PAR_2 or a downstream mediator, such as TRP channels. TRPV1 is a downstream target of PAR_2 that contributes to the effects of proteases on inflammation and nociception (Amadesi *et al.*, 2004, Dai 2004). Capsaicin directly activates TRPV1 on primary sensory neurons to cause neurogenic inflammation and pain (Caterina *et al.*, 1997). We examined whether GB88 affects capsaicin-induced inflammation and nociception. Intraplantar injection of capsaicin evoked a 54.8 ± 3.7% increase in paw thickness within 1 h that was persistent for 4 h (Fig. 4A). Capsaicin also induced a robust mechanical hyperalgesia at 1 h that was sustained for 4 h (Fig. 4B). GB88 had no effects on capsaicin-stimulated oedema and mechanical hyperalgesia (Fig. 4A, B). Thus, the anti-inflammatory and analgesic actions of GB88 are not due to antagonism of TRPV1, since the proinflammatory and nociceptive effects of capsaicin were unaffected.

Effects of GB88 on inflammation and pain in PAR_2-deficient mice. *Par_2* deletion attenuates the effects of trypsin, Cat-S and elastase on oedema and hyperalgesia (Vergnolle *et al.*, 2001; Zhao *et al.*, 2014a; Zhao *et al.*, 2015). Since *Par_2* deletion does not completely inhibit Cat-S-evoked inflammation and pain (Zhao *et al.*, 2014a), we examined whether GB88 has residual actions in *$Par_2^{-/-}$* mice, which could suggest additional actions that are unrelated to PAR_2 antagonism. In wild-type mice, Cat-S evoked an 18.7± 3.2% increase paw thickness (Fig. 5 A) and a sustained mechanical hyperalgesia (Fig. 5 B). GB88 reduced Cat-S-induced

oedema and hyperalgesia. GB88 inhibited Cat-S-evoked oedema and mechanical hyperalgesia to the same extent in $Par_2^{+/+}$ and $Par_2^{-/-}$ mice. The inability of GB88 to exert additional anti-inflammatory and antinociceptive effects in $Par_2^{-/-}$ mice suggests the actions of GB88 are mediated by antagonism of PAR_2.

Expression of PAR_2 in nociceptors. Proteases can evoke neurogenic inflammation and pain directly by activating PAR_2 on primary sensory neurons (Steinhoff *et al.*, 2000), or indirectly by releasing stimulants from keratinocytes, which express high levels of PAR_2 (Steinhoff *et al.*, 1999). We used *in situ* hybridization to examine the expression of PAR_2 mRNA by the primary sensory neurons in dorsal root and trigeminal ganglia of rat and mouse. In mouse, PAR_2 was detected at low levels in DRG neurons (data not shown), but was more prominently expressed in trigeminal neurons (Fig. 6A). In rat, PAR_2 mRNA was readily detected in DRG neurons (Fig. 6B, C). PAR_2-positive neurons were small diameter, and included peptidergic neurons expressing immunoreactive CGRP and non-peptidergic neurons that bound IB4 (Fig. 6C-G). PAR_2-positive neurons did not express NF200, a marker for large diameter neurons. Thus, PAR_2 is present in rat nociceptors.

GB88 antagonism of activation of nociceptors by canonical and biased protease agonists of PAR_2. To determine whether GB88 can attenuate the actions of canonical and biased proteases on nociceptors, we examined protease-evoked Ca^{2+} signaling in DRG neurons in short-term culture. We studied neurons from rats rather than mice due to the higher expression of PAR_2 in rat nociceptors (Fig. 6) and because PAR_2 agonists generated larger signals in a higher proportion of DRG neurons from rats than mice (not shown). We have previously reported that canonical (trypsin, tryptase) and biased (Cat-S, elastase) can evoke PAR_2-dependent Ca^{2+} signals in DRG neurons (Steinhoff *et al.*, 2000; Zhao *et al.*, 2014a; Zhao *et al.*, 2015). However, whereas canonical proteases evoke PAR_2 coupling to Gαq and mobilization of intracellular Ca^{2+}, Cat-S- and elastase-activated PAR_2 does not couple to Gαq, and instead causes Gαs-, adenylyl cyclase- and PKA-mediated activation of TRPV4, which permits influx of Ca^{2+} ions form the extracellular fluid (Zhao *et al.*, 2014a; Zhao *et al.*, 2015).

Trypsin induced a rapid but transient increase in $[Ca^{2+}]_i$ that was maximal at 2 min and return to baseline after 5 min, consistent with mobilization of Ca^{2+} ions from intracellular stores (Fig. 7 A). Cat-S and elastase caused a gradual and sustained increased $[Ca^{2+}]_i$ that was maintained for at least 5 min, which is consistent with activation of TRPV4 and influx of extracellular Ca^{2+} ions (Fig. 7, C, F). GB88 markedly inhibited the magnitude of responses to trypsin, Cat-S and elastase. Of all the capsaicin- and KCl-responsive neurons, 52 ± 5% responded to trypsin, 49 ± 7% responded to Cat-S, and 57 ± 10% responded to elastase. GB88 reduced the proportion of responsive neurons by >60% (Fig. 7 G). In contrast, GB88 neither affected the magnitude of the Ca^{2+} response to capsaicin nor the proportion of capsaicin-responsive neurons, consistent with its inability to inhibit capsaicin-evoked inflammation and pain. Our results suggest that GB88 inhibits proteolytic activation of nociceptive neurons, which we have shown depends in large part of PAR_2 (Zhao *et al.*, 2014a; Zhao *et al.*, 2015).

Effects of GB88 on protease activity. To eliminate the possibility that the analgesic effects of GB88 were mediated by direct protease inhibition rather than PAR_2 antagonism, we studied the ability of GB88 to prevent proteolytic activity. Using fluorogenic substrates, we monitored the activity of recombinant proteases upon initial interaction with GB88, mimicking the conditions that were used in the studies of DRG neurons. GB88 (1, 10, 100 μM) did not affect the activity of trypsin or elastase, but moderately reduced Cat-S activity (<20% inhibition; Fig. 8A). We also tested the ability of GB88 to inhibit the binding of proteases to covalent activity-based probes (Fig. 8B, C). In this assay, GB88 was incubated with the enzyme for 30 min. Trypsin activity was not affected at any concentration of GB88 tested (1, 10, 100 μM). Cat-S and elastase activities were modestly affected at 10 μM (<25% inhibition) and more so at 100 μM GB88 (40% and 74%, respectively). Hence, GB88 can directly inhibit proteases activity, but only at high concentrations, which are unlikely to be achieved *in vivo*. Thus, the effects of GB88 on nociceptor activation, inflammation and pain are unlikely to be due to direct effects on protease activity, but rather through antagonism of PAR_2.

DISCUSSION & CONCLUSIONS

We report that GB88, a small molecule PAR_2 antagonist, inhibits the capacity of canonical and biased proteases to activate PAR_2 on nociceptors and cause inflammation and pain. GB88 inhibited the activation of nociceptors by trypsin, Cat-S and elastase, and suppressed the proinflammatory and pronociceptive actions of these proteases.

GB88 inhibits the proinflammatory and pronociceptive actions of canonical and biased agonists of PAR_2. Our results show that GB88 inhibits the proinflammatory and pronociceptive actions of proteases that are canonical and biased agonists of PAR_2. Trypsin, a canonical agonist, cleaves at $Arg^{36}\downarrow Ser^{37}$, and activates PAR_2 by a tethered ligand mechanism (Bohm *et al.*, 1996; Nystedt *et al.*, 1995; Nystedt *et al.*, 1994). Trypsin-activated PAR_2 couples to Gαq, which mobilizes intracellular calcium, and recruits β-arrestins, leading to receptor endocytosis (Ayoub *et al.*, 2013; DeFea *et al.*, 2000; Dery *et al.*, 1999). Cat-S and elastase activate PAR_2 by different mechanisms. Cat-S cleaves at $Glu^{56}\downarrow Thr^{5}$, which reveals a unique tethered ligand (Zhao *et al.*, 2014a). Elastase cleaves at $Ser^{67}\downarrow Val^{68}$, and activates PAR_2 by a mechanism that does not involve tethered ligand binding (Ramachandran *et al.*, 2011; Zhao *et al.*, 2015). Cat-S- and elastase-cleaved PAR_2 couples to Gαs, but not Gαq or β-arrestins, and elastase-cleaved PAR_2 also couples to Gα12/13. Thus, Cat-S and elastase are biased agonists of PAR_2. Despite these divergent mechanisms of PAR_2 activation and signaling, trypsin, Cat-S and elastase all cause PAR_2-dependent inflammation and pain (Steinhoff *et al.*, 2000; Vergnolle *et al.*, 2001; Zhao *et al.*, 2014a; Zhao *et al.*, 2015). However, whereas trypsin causes PKC- and PKA-dependent sensitization of TRP channels and nociceptors, Cat-S and elastase activate TRP channels and nociceptors solely *via* PKA (Amadesi *et al.*, 2006; Zhao *et al.*, 2014a; Zhao *et al.*, 2015).

We found that trypsin, Cat-S or elastase caused sustained oedema and mechanical hyperalgesia in mice. Trypsin and Cat-S, but not elastase, also caused thermal hyperalgesia. The reason for the differences in the tendency of proteases to cause thermal hyperalgesia is unknown, but may relate to the activation of different signaling processes that differentially sensitize thermo-sensitive TRP channels. Although trypsin, Cat-S and elastase induce PAR_2-

dependent activation of TRPV4 (Zhao *et al.*, 2014a; Zhao *et al.*, 2015), trypsin can also sensitize TRPV1 and TRPA1 (Amadesi *et al.*, 2004; Dai *et al.*, 2004; Dai *et al.*, 2007). Further studies are required to ascertain whether Cat-S and elastase can sensitize TRPV1 and TRPA1.

GB88 inhibited the proinflammatory and pronociceptive actions of trypsin, Cat-S and elastase. These results are consistent with the observation that *Par*$_2$ deletion inhibits trypsin-, Cat-S- and elastase evoked inflammation and pain (Vergnolle *et al.*, 2001; Zhao *et al.*, 2014a; Zhao *et al.*, 2015). GB88 did not affect capsaicin-evoked and TRPV1-mediated inflammation and pain, and had no additional anti-inflammatory of algesic actions in *Par*$_2$ deficient mice, which suggest that PAR_2 is the primary target of GB88 *in vivo*. Minor differences in the degree to which GB88 inhibited the proinflammatory and pronociceptive effects of proteases may be attributable to different mechanisms of action. Although PAR_2 plays a dominant role in protease-evoked inflammation and pain, elastase also activates PAR_1 (Mihara *et al.*, 2013), and Cat-S cleaves and activates MrgprC11 (Reddy *et al.*, 2015).

GB88 inhibited the proinflammatory and pronociceptive actions of the PAR_2 agonists 2-furoyl-LIGRLO-NH_2 and AC264613. 2-furoyl-LIGRLO-NH_2 and AC264613 are selective for PAR_2 over other PARs, and induce oedema and hyperalgesia after intraplantar injection (Gardell *et al.*, 2008; Kanke *et al.*, 2005; Suen *et al.*, 2012). In support of these observations, we found that GB88 prevented 2-furoyl-LIGRLO-NH_2- and AC264613-induced oedema and mechanical hyperalgesia in mice. These results are consistent with our observation that GB88 also inhibited protease-evoked inflammation and pain, and support the view that GB88 exerts anti-inflammatory and analgesic actions by antagonism of PAR_2.

GB88 inhibits the activation of nociceptors by canonical and biased agonists of PAR_2. Our results show that GB88 blocked the capacity of proteases that activate PAR_2 by canonical and biased mechanisms to activate nociceptors. PAR_2 mRNA was readily detected in rat DRG neurons by *in situ* hybridization. PAR_2-positive neurons were small diameter, and included peptidergic and non-peptidergic neurons with the characteristics of nociceptors. Our findings support other reports of prominent expression of PAR_2 in nociceptors (Steinhoff *et*

al., 2000; Vellani *et al.*, 2010). Consistent with these findings, trypsin, Cat-S and elastase induced robust increases in $[Ca^{2+}]_i$ in a substantial proportion of small diameter, capsaicin-sensitive rat DRG neurons. Whereas trypsin stimulated a rapid and transient increase in $[Ca^{2+}]_i$, consistent with mobilization of intracellular calcium stores, Cat-S and elastase induced a gradual and sustained increase in $[Ca^{2+}]_i$, which suggests activation of a plasma membrane channel and influx of extracellular Ca^{2+} ions. Regardless of the mechanism, GB88 inhibited the magnitude of protease-evoked calcium signals and the proportion of neurons with detectable responses. Thus, PAR_2 is a prominent mediator of protease signaling to nociceptive neurons. Residual responses in GB88-treated neurons may be attributed to activation of other receptors or channels. Elastase can also activate PAR_1, and Cat-S activates MrgprC11, which are expressed in nociceptors (Mihara *et al.*, 2013; Reddy *et al.*, 2015; Vellani *et al.*, 2010).

PAR_2 mRNA was less prominent in DRG and trigeminal neurons of mice. Although trypsin, Cat-S and elastase cause PAR_2-mediated activation of mouse nociceptors, assessed by measurement of excitability and calcium signals (Amadesi *et al.*, 2006; Zhao *et al.*, 2014a; Zhao *et al.*, 2015), there are fewer responsive neurons in mouse than rat. Whereas trypsin evokes a rapid increase in $[Ca^{2+}]_i$ in mouse nociceptors, Cat-S and elastase induce a gradual and sustained increase in $[Ca^{2+}]_i$. These differences are attributable to the divergent mechanisms by which these proteases activate PAR_2. Trypsin-activated PAR_2 couples to Gαs and mobilization of intracellular calcium, but Cat-S- and elastase-activated PAR_2 is unable to couple to Gαq and does not mobilize intracellular calcium (Zhao *et al.*, 2014a; Zhao *et al.*, 2015). Instead, Cat-S- and elastase-activated PAR_2 couples to Gαs, adenylyl cyclase and cAMP, and induces a PKA-dependent activation of TRPV4 and influx of extracellular calcium ions. Trypsin-activated PAR_2 stimulates TRPV4 by PKC- and tyrosine-kinase mechanisms.

GB88 mechanism and selectivity. GB88 inhibited the ability of canonical and biased agonists of PAR_2 to activate nociceptors and cause inflammation and pain. GB88 inhibits PAR_2 activation in cell lines by trypsin, Cat-S and 2-furoyl-LIGRLO-NH_2, and is a competitive

and surmountable antagonist of 2-furoyl-LIGRLO-NH_2 (Suen *et al.*, 2012; Zhao *et al.*, 2014a). Trypsin, Cat-S and elastase cleave PAR_2 at different sites. Trypsin and Cat-S cleavage revealed distinct tethered ligands, whereas elastase activates PAR_2 by a non-tethered ligand mechanism. Thus, GB88 binding most probably antagonises PAR_2 by stabilizing inactive conformations rather than by inhibiting cleavage or binding of a specific tethered ligand. GB88 is a pathway-selective antagonist of PAR_2, showing preference for antagonism of Gαq signaling and agonism of Gαi/o signaling (Suen *et al.*, 2014), which may account for its ability to antagonise the actions of Cat-S and elastase. Further studies are required to define the mechanisms by which GB88 inhibits Cat-S and elastase activation of PAR_2.

TRP channels are downstream targets of PAR_2. PAR_2 can sensitize TRPV1, and TRPV1 deletion or antagonism inhibits PAR_2-dependent hyperalgesia (Amadesi *et al.*, 2004, Dai 2004). We found that GB88 did not affect capsaicin-evoked calcium signals in nociceptors, consistent with its inability to inhibit the proinflammatory and algesic actions of capsaicin. These findings support the conclusion that GB88 prevents protease-activation of nociceptors, inflammation and pain by antagonism of PAR_2 rather than TRPV1.

To confirm that the effects of GB88 were not due to protease inhibition, we examined whether GB88 inhibits protease activity. By using a fluorogenic assay to mimic conditions of protease signaling to nociceptors in culture, we found that GB88 (10 μM) did not affect trypsin or elastase activity, and had a modest effect on Cat-S activity. When pre-incubated with activity-based probes, GB88 did not affect trypsin binding, and inhibited Cat-S and elastase binding only at high concentrations (>10 μM) that are likely to exceed those attained *in vivo*. Thus, the effects of GB88 on inflammation and pain are more likely due to antagonism of PAR_2 rather than inhibition of protease activity.

Multiple proteases become activated during injury and inflammation, when the balance of protease activation and levels of endogenous inhibitors is crucially important for inflammatory and neuropathic pain. Cat-S is activated in macrophages and spinal microglial cells during colitis and in neuropathic pain states (Cattaruzza *et al.*, 2011; Clark *et al.*, 2007), and mast cell tryptase is elevated in patients with visceral pain (Barbara *et al.*, 2004).

Elastase released from leukocytes within sensory ganglia can contribute to neuropathic pain, which is exacerbated by deficiency in the elastase inhibitor serpinA3N (Vicuna *et al.*, 2015). Thus, our finding that GB88 inhibits the pronociceptive actions of diverse proteases suggests its potential to suppress different forms of inflammatory and neuropathic pain that are associated with the differential activation of proteases. Our findings expand the usefulness of GB88 and related compounds to inhibit inflammatory and painful conditions (Barry *et al.*, 2010; Lohman *et al.*, 2012a; Lohman *et al.*, 2012b; Suen *et al.*, 2012; Zhao *et al.*, 2014a).

AUTHORS' CONTRIBUTIONS. TML and ES analysed pain and inflammation. PZ and DPP studied nociceptor activation. RB localised receptors by *in situ* hybridization. LEM analysed the enzymatic activity. RL and DF provided GB88 and conceived the studies of pain. TM and NWB wrote the manuscript. NWB designed the study and oversaw the project.

ACKNOWLEDGEMENTS. Supported by National Health and Medical Research Council, Australian Research Council Centre of Excellence in Convergent Bio-Nano Science and Technology and Monash University. Work in the authors' laboratory is funded in part by Takeda Pharmaceuticals Inc.

REFERENCES

Alemi F, Kwon E, Poole DP, Lieu T, Lyo V, Cattaruzza F*, et al.* (2013). The TGR5 receptor mediates bile acid-induced itch and analgesia. *The Journal of clinical investigation* 123: 1513-1530.

Amadesi S, Cottrell GS, Divino L, Chapman K, Grady EF, Bautista F*, et al.* (2006). Protease-activated receptor 2 sensitizes TRPV1 by protein kinase Cepsilon- and A-dependent mechanisms in rats and mice. *J Physiol* 575: 555-571.

Amadesi S, Grant AD, Cottrell GS, Vaksman N, Poole DP, Rozengurt E*, et al.* (2009). Protein kinase D isoforms are expressed in rat and mouse primary sensory neurons and are activated by agonists of protease-activated receptor 2. *J Comp Neurol* 516: 141-156.

Amadesi S, Nie J, Vergnolle N, Cottrell GS, Grady EF, Trevisani M*, et al.* (2004). Protease-activated receptor 2 sensitizes the capsaicin receptor transient receptor potential vanilloid receptor 1 to induce hyperalgesia. *J Neurosci* 24: 4300-4312.

Ayoub MA, Pin JP (2013). Interaction of Protease-Activated Receptor 2 with G Proteins and beta-Arrestin 1 Studied by Bioluminescence Resonance Energy Transfer. *Front Endocrinol (Lausanne)* 4: 196.

Barbara G, Stanghellini V, De Giorgio R, Cremon C, Cottrell GS, Santini D*, et al.* (2004). Activated mast cells in proximity to colonic nerves correlate with abdominal pain in irritable bowel syndrome. *Gastroenterology* 126: 693-702.

Barry GD, Suen JY, Le GT, Cotterell A, Reid RC, Fairlie DP (2010). Novel agonists and antagonists for human protease activated receptor 2. *J Med Chem* 53: 7428-7440.

Bohm SK, Kong W, Bromme D, Smeekens SP, Anderson DC, Connolly A*, et al.* (1996). Molecular cloning, expression and potential functions of the human proteinase-activated receptor-2. *Biochem J* 314 (Pt 3): 1009-1016.

Boitano S, Hoffman J, Flynn AN, Asiedu MN, Tillu DV, Zhang Z*, et al.* (2015). The novel PAR2 ligand C391 blocks multiple PAR2 signalling pathways in vitro and in vivo. *British journal of pharmacology*.

Bron R, Wood RJ, Brock JA, Ivanusic JJ (2014). Piezo2 expression in corneal afferent neurons. *J Comp Neurol* 522: 2967-2979.

Caterina MJ, Schumacher MA, Tominaga M, Rosen TA, Levine JD, Julius D (1997). The capsaicin receptor: a heat-activated ion channel in the pain pathway. *Nature* 389: 816-824.

Cattaruzza F, Lyo V, Jones E, Pham D, Hawkins J, Kirkwood K*, et al.* (2011). Cathepsin S is activated during colitis and causes visceral hyperalgesia by a PAR2-dependent mechanism in mice. *Gastroenterology* 141: 1864-1874 e1861-1863.

Chaplan SR, Bach FW, Pogrel JW, Chung JM, Yaksh TL (1994). Quantitative assessment of tactile allodynia in the rat paw. *J Neurosci Methods* 53: 55-63.

Clark AK, Yip PK, Grist J, Gentry C, Staniland AA, Marchand F*, et al.* (2007). Inhibition of spinal microglial cathepsin S for the reversal of neuropathic pain. *Proc Natl Acad Sci U S A* 104: 10655-10660.

Corvera CU, Dery O, McConalogue K, Bohm SK, Khitin LM, Caughey GH*, et al.* (1997). Mast cell tryptase regulates rat colonic myocytes through proteinase-activated receptor 2. *The Journal of clinical investigation* 100: 1383-1393.

Cottrell GS, Amadesi S, Pikios S, Camerer E, Willardsen JA, Murphy BR*, et al.* (2007). Protease-activated receptor 2, dipeptidyl peptidase I, and proteases mediate Clostridium difficile toxin A enteritis. *Gastroenterology* 132: 2422-2437.

Dai Y, Moriyama T, Higashi T, Togashi K, Kobayashi K, Yamanaka H*, et al.* (2004). Proteinase-activated receptor 2-mediated potentiation of transient receptor potential vanilloid subfamily 1 activity reveals a mechanism for proteinase-induced inflammatory pain. *J Neurosci* 24: 4293-4299.

Dai Y, Wang S, Tominaga M, Yamamoto S, Fukuoka T, Higashi T*, et al.* (2007). Sensitization of TRPA1 by PAR2 contributes to the sensation of inflammatory pain. *The Journal of clinical investigation* 117: 1979-1987.

DeFea KA, Zalevsky J, Thoma MS, Dery O, Mullins RD, Bunnett NW (2000). beta-arrestin-dependent endocytosis of proteinase-activated receptor 2 is required for intracellular targeting of activated ERK1/2. *The Journal of cell biology* 148: 1267-1281.

Dery O, Thoma MS, Wong H, Grady EF, Bunnett NW (1999). Trafficking of proteinase-activated receptor-2 and beta-arrestin-1 tagged with green fluorescent protein. beta-Arrestin-dependent endocytosis of a proteinase receptor. *The Journal of biological chemistry* 274: 18524-18535.

Dulon S, Cande C, Bunnett NW, Hollenberg MD, Chignard M, Pidard D (2003). Proteinase-activated receptor-2 and human lung epithelial cells: disarming by neutrophil serine proteinases. *Am J Respir Cell Mol Biol* 28: 339-346.

Elmariah SB, Reddy VB, Lerner EA (2014). Cathepsin S signals via PAR2 and generates a novel tethered ligand receptor agonist. *PLoS One* 9: e99702.

Ferrell WR, Lockhart JC, Kelso EB, Dunning L, Plevin R, Meek SE*, et al.* (2003). Essential role for proteinase-activated receptor-2 in arthritis. *The Journal of clinical investigation* 111: 35-41.

Gardell LR, Ma JN, Seitzberg JG, Knapp AE, Schiffer HH, Tabatabaei A*, et al.* (2008). Identification and characterization of novel small-molecule protease-activated receptor 2 agonists. *J Pharmacol Exp Ther* 327: 799-808.

Gilmore BF, Quinn DJ, Duff T, Cathcart GR, Scott CJ, Walker B (2009). Expedited solid-phase synthesis of fluorescently labeled and biotinylated aminoalkane diphenyl phosphonate affinity probes for chymotrypsin- and elastase-like serine proteases. *Bioconjugate chemistry* 20: 2098-2105.

Goh FG, Ng PY, Nilsson M, Kanke T, Plevin R (2009). Dual effect of the novel peptide antagonist K-14585 on proteinase-activated receptor-2-mediated signalling. *British journal of pharmacology* 158: 1695-1704.

Grant AD, Cottrell GS, Amadesi S, Trevisani M, Nicoletti P, Materazzi S*, et al.* (2007). Protease-activated receptor 2 sensitizes the transient receptor potential vanilloid 4 ion channel to cause mechanical hyperalgesia in mice. *J Physiol* 578: 715-733.

Hargreaves K, Dubner R, Brown F, Flores C, Joris J (1988). A new and sensitive method for measuring thermal nociception in cutaneous hyperalgesia. *Pain* 32: 77-88.

Hollenberg MD, Mihara K, Polley D, Suen JY, Han A, Fairlie DP*, et al.* (2014). Biased signalling and proteinase-activated receptors (PARs): targeting inflammatory disease. *British journal of pharmacology* 171: 1180-1194.

Jacob C, Yang PC, Darmoul D, Amadesi S, Saito T, Cottrell GS*, et al.* (2005). Mast cell tryptase controls paracellular permeability of the intestine. Role of protease-activated receptor 2 and beta-arrestins. *The Journal of biological chemistry* 280: 31936-31948.

Jensen DD, Godfrey CB, Niklas C, Canals M, Kocan M, Poole DP*, et al.* (2013). The bile acid receptor TGR5 does not interact with beta-arrestins or traffic to endosomes but transmits sustained signals from plasma membrane rafts. *The Journal of biological chemistry* 288: 22942-22960.

Kanke T, Ishiwata H, Kabeya M, Saka M, Doi T, Hattori Y*, et al.* (2005). Binding of a highly potent protease-activated receptor-2 (PAR2) activating peptide, [3H]2-furoyl-LIGRL-NH2, to human PAR2. *British journal of pharmacology* 145: 255-263.

Kelso EB, Lockhart JC, Hembrough T, Dunning L, Plevin R, Hollenberg MD*, et al.* (2006). Therapeutic promise of proteinase-activated receptor-2 antagonism in joint inflammation. *J Pharmacol Exp Ther* 316: 1017-1024.

Lieu T, Jayaweera G, Zhao P, Poole DP, Jensen D, Grace M*, et al.* (2014). The bile acid receptor TGR5 activates the TRPA1 channel to induce itch in mice. *Gastroenterology* 147: 1417-1428.

Lindner JR, Kahn ML, Coughlin SR, Sambrano GR, Schauble E, Bernstein D*, et al.* (2000). Delayed onset of inflammation in protease-activated receptor-2-deficient mice. *J Immunol* 165: 6504-6510.

Lohman RJ, Cotterell AJ, Barry GD, Liu L, Suen JY, Vesey DA*, et al.* (2012a). An antagonist of human protease activated receptor-2 attenuates PAR2 signaling, macrophage activation, mast cell degranulation, and collagen-induced arthritis in rats. *FASEB J* 26: 2877-2887.

Lohman RJ, Cotterell AJ, Suen J, Liu L, Do AT, Vesey DA*, et al.* (2012b). Antagonism of protease-activated receptor 2 protects against experimental colitis. *J Pharmacol Exp Ther* 340: 256-265.

Mihara K, Ramachandran R, Renaux B, Saifeddine M, Hollenberg MD (2013). Neutrophil elastase and proteinase-3 trigger G protein-biased signaling through proteinase-activated receptor-1 (PAR1). *The Journal of biological chemistry* 288: 32979-32990.

Nystedt S, Emilsson K, Larsson AK, Strombeck B, Sundelin J (1995). Molecular cloning and functional expression of the gene encoding the human proteinase-activated receptor 2. *Eur J Biochem* 232: 84-89.

Nystedt S, Emilsson K, Wahlestedt C, Sundelin J (1994). Molecular cloning of a potential proteinase activated receptor. *Proc Natl Acad Sci U S A* 91: 9208-9212.

Ossovskaya VS, Bunnett NW (2004). Protease-activated receptors: contribution to physiology and disease. *Physiol Rev* 84: 579-621.

Pan Z, Jeffery DA, Chehade K, Beltman J, Clark JM, Grothaus P*, et al.* (2006). Development of activity-based probes for trypsin-family serine proteases. *Bioorganic & medicinal chemistry letters* 16: 2882-2885.

Poole DP, Amadesi S, Veldhuis NA, Abogadie FC, Lieu T, Darby W*, et al.* (2013). Protease-activated receptor 2 (PAR2) protein and transient receptor potential vanilloid 4 (TRPV4) protein coupling is required for sustained inflammatory signaling. *The Journal of biological chemistry* 288: 5790-5802.

Ramachandran R, Mihara K, Chung H, Renaux B, Lau CS, Muruve DA*, et al.* (2011). Neutrophil elastase acts as a biased agonist for proteinase-activated receptor-2 (PAR2). *The Journal of biological chemistry* 286: 24638-24648.

Reddy VB, Sun S, Azimi E, Elmariah SB, Dong X, Lerner EA (2015). Redefining the concept of protease-activated receptors: cathepsin S evokes itch via activation of Mrgprs. *Nature communications* 6: 7864.

Schmidlin F, Amadesi S, Dabbagh K, Lewis DE, Knott P, Bunnett NW*, et al.* (2002). Protease-activated receptor 2 mediates eosinophil infiltration and hyperreactivity in allergic inflammation of the airway. *J Immunol* 169: 5315-5321.

Shichijo M, Kondo S, Ishimori M, Watanabe S, Helin H, Yamasaki T*, et al.* (2006). PAR-2 deficient CD4+ T cells exhibit downregulation of IL-4 and upregulation of IFN-gamma after antigen challenge in mice. *Allergol Int* 55: 271-278.

Steinhoff M, Corvera CU, Thoma MS, Kong W, McAlpine BE, Caughey GH*, et al.* (1999). Proteinase-activated receptor-2 in human skin: tissue distribution and activation of keratinocytes by mast cell tryptase. *Experimental dermatology* 8: 282-294.

Steinhoff M, Vergnolle N, Young SH, Tognetto M, Amadesi S, Ennes HS*, et al.* (2000). Agonists of proteinase-activated receptor 2 induce inflammation by a neurogenic mechanism. *Nature medicine* 6: 151-158.

Suen JY, Barry GD, Lohman RJ, Halili MA, Cotterell AJ, Le GT*, et al.* (2012). Modulating human proteinase activated receptor 2 with a novel antagonist (GB88) and agonist (GB110). *British journal of pharmacology* 165: 1413-1423.

Suen JY, Cotterell A, Lohman RJ, Lim J, Han A, Yau MK*, et al.* (2014). Pathway-selective antagonism of proteinase activated receptor 2. *British journal of pharmacology* 171: 4112-4124.

Vellani V, Kinsey AM, Prandini M, Hechtfischer SC, Reeh P, Magherini PC*, et al.* (2010). Protease activated receptors 1 and 4 sensitize TRPV1 in nociceptive neurones. *Molecular pain* 6: 61.

Verdoes M, Oresic Bender K, Segal E, van der Linden WA, Syed S, Withana NP*, et al.* (2013). Improved quenched fluorescent probe for imaging of cysteine cathepsin activity. *Journal of the American Chemical Society* 135: 14726-14730.

Vergnolle N, Bunnett NW, Sharkey KA, Brussee V, Compton SJ, Grady EF*, et al.* (2001). Proteinase-activated receptor-2 and hyperalgesia: A novel pain pathway. *Nature medicine* 7: 821-826.

Vicuna L, Strochlic DE, Latremoliere A, Bali KK, Simonetti M, Husainie D*, et al.* (2015). The serine protease inhibitor SerpinA3N attenuates neuropathic pain by inhibiting T cell-derived leukocyte elastase. *Nature medicine* 21: 518-523.

Wang H, Moreau F, Hirota CL, MacNaughton WK (2010). Proteinase-activated receptors induce interleukin-8 expression by intestinal epithelial cells through ERK/RSK90 activation and histone acetylation. *FASEB J* 24: 1971-1980.

Wang H, Wen S, Bunnett NW, Leduc R, Hollenberg MD, MacNaughton WK (2008). Proteinase-activated receptor-2 induces cyclooxygenase-2 expression through beta-catenin and cyclic AMP-response element-binding protein. *The Journal of biological chemistry* 283: 809-815.

Zhao P, Lieu T, Barlow N, Metcalf M, Veldhuis NA, Jensen DD*, et al.* (2014a). Cathepsin S causes inflammatory pain via biased agonism of PAR2 and TRPV4. *The Journal of biological chemistry* 289: 27215-27234.

Zhao P, Lieu T, Barlow N, Sostegni S, Haerteis S, Korbmacher C*, et al.* (2015). Neutrophil Elastase Activates Protease-activated Receptor-2 (PAR2) and Transient Receptor Potential

Vanilloid 4 (TRPV4) to Cause Inflammation and Pain. *The Journal of biological chemistry* 290: 13875-13887.

Zhao P, Metcalf M, Bunnett NW (2014b). Biased signaling of protease-activated receptors. *Front Endocrinol (Lausanne)* 5: 67.

FIGURE LEGENDS

Figure 1. Effects of GB88 on protease-evoked inflammation and pain. Mice were treated with GB88 (10 mg/kg p.o.) or vehicle 2 h before intraplantar injections of trypsin (**A-C**, 30 ng), Cat-S (**D-F**, 14 µg), elastase (**G-I**, 290 ng) or vehicle. Paw thickness (**A, D, G**), paw withdrawal to mechanical stimulation (**B, E, H**), and paw withdrawal to thermal stimulation (**C, F, I**) were measured. *P<0.05, **P<0.01, ***P<0.001, ****P<0.0001 compared to vehicle/vehicle control.

Figure 2. Effects of GB88 on basal inflammation and pain. Mice were treated with GB88 (10 mg/kg p.o.) or vehicle 2 h before intraplantar injection of vehicle. Paw thickness (**A**) and paw withdrawal to mechanical stimulation (**B**) were measured hourly for 4 h.

Figure 3. Effects of GB88 on PAR_2 agonist-evoked inflammation and pain. Mice were treated with GB88 (10 mg/kg p.o.) or vehicle 2 h before intraplantar injections of 2-furoyl-LIGRLO-NH_2 (2F) (**A, B**, 500 ng) or AC264613 (**C, D**, 1 µg). Paw thickness (**A, C**) and paw withdrawal to mechanical stimulation (**B, D**) were measured hourly for 4 h. *P<0.05, **P<0.01, ***P<0.001, ****P<0.0001 compared to vehicle/vehicle control.

Figure 4. Effects of GB88 on capsaicin-evoked inflammation and pain. Mice were treated with GB88 (10 mg/kg p.o.) or vehicle 2 h before intraplantar injection of capsaicin (Cap, 5 µg). Paw thickness (**A**) and paw withdrawal to mechanical stimulation (**B**) were measured hourly for 4 h. **P<0.01, ***P<0.001, ****P<0.0001 compared to vehicle/Cat-S control.

Figure 5. Effects of GB88 on inflammation and pain in PAR_2 deficient mice. $Par_2^{+/+}$ (wild-type, WT) or $Par_2^{-/-}$ (knockout, KO) mice were treated with GB88 (10 mg/kg p.o.) or vehicle 2 h before intraplantar injection of Cat-S (14 µg). Paw thickness (**A**) and paw withdrawal to mechanical stimulation (**B**) were measured hourly for 4 h. ****P<0.0001 compared to vehicle/vehicle control.

Figure 6. Localization of PAR_2 mRNA in DRG. *In situ* hybridisation on sections of mouse trigeminal (**A**) ganglia or rat DRG (**B**). **C-G**. The inset shows an inverted image of PAR_2 in situ hybridization (ISH, **C**), immunoreactive CGRP (**D**), immunoreactive neurofilament 200

(NF200, **E**), IB4 (**F**), and a merged image (**G**). Arrow heads show expression of PAR_2 in small diameter neurons that expressed CGRP or bound IB4. Scale, 20 μm.

Figure 7. Effects of GB88 on protease-evoked Ca^{2+} signaling in DRG neurons. Rat DRG neurons were challenged with trypsin (**A, B**, 10 nM), elastase (**C, D**, 100 nM) or Cat-S (**E, F**, 100 nM) in the presence of GB88 (10 μM) or vehicle (control). **A, C, E.** Representative traces of kinetics of Ca^{2+} responses. **B, D, F**. Area under the curve (AUC) from 50-250 s. **G**. Effects of GB88 on the proportion of protease-responsive neurons that also responded to capsaicin. *P<0.05, ***P<0.001. n=4-6 rats, with >100 neurons analysed from each rat.

Figure 8. Effects of GB88 on protease activity. A. Effects of GB88 on protease cleavage of fluorogenic substrates. GB88 (10 μM) was mixed with substrates (50 μM). Proteases were added (final concentrations: trypsin, 10 nM; Cat-S, 100 nM; elastase, 100 nM) and fluorescence was monitored. The slope of the reaction was measured during the initial 60-120 s (in the linear range). **B, C.** Effects of GB88 on protease labelling by fluorescent activity-based probes. Recombinant proteases were pre-treated with GB88 (1, 10, 100 μM) in 1% DMSO. Residual activity was determined by labelling with activity-based probes and analysis by fluorescent SDS-PAGE. B shows a representative gel. C shows quantified signals. **P<0.01, n=5 or 6 separate experiments.

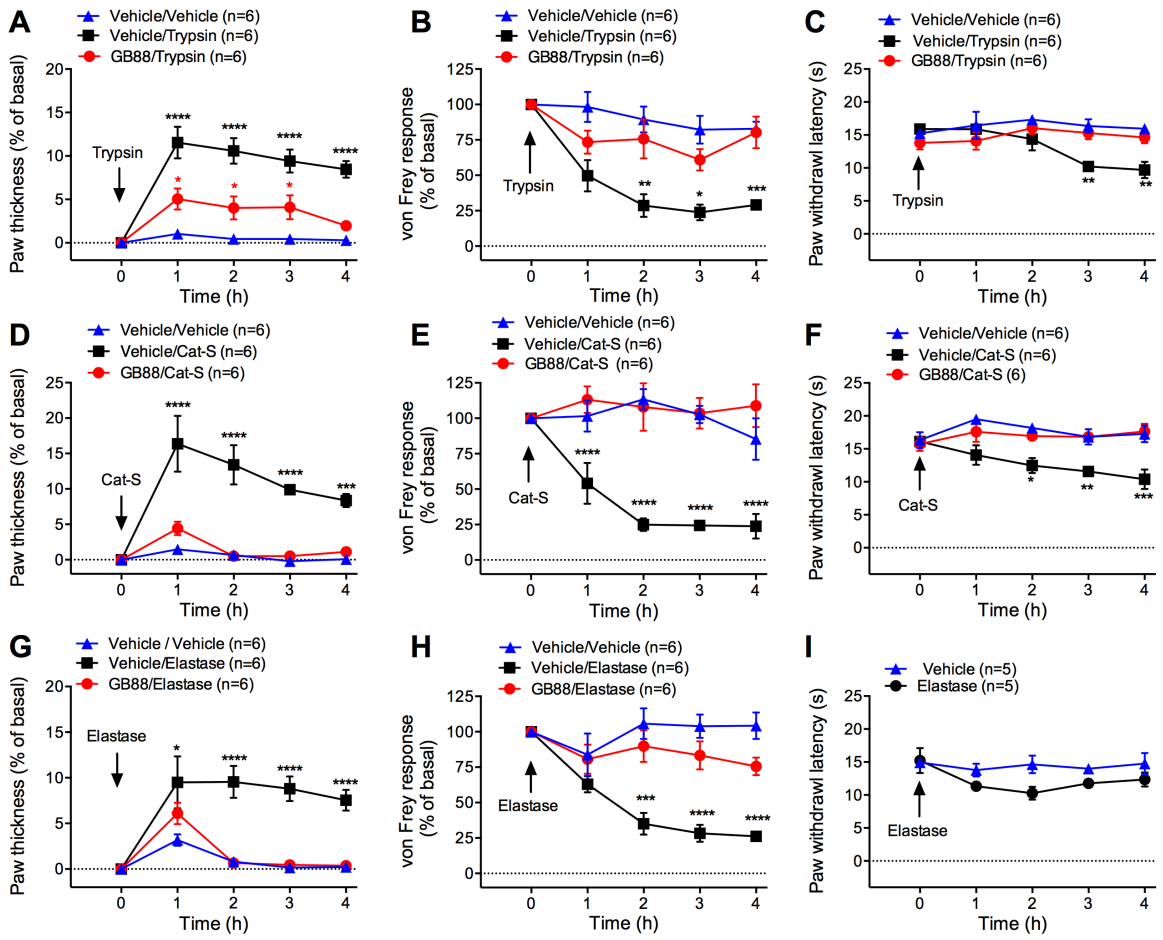
A
Vehicle/Vehicle (n=6)
Vehicle/Trypsin (n=6)
GB88/Trypsin (n=6)
Paw thickness (% of basal)
Trypsin
Time (h)
B
Vehicle/Vehicle (n=6)
Vehicle/Trypsin (n=6)
GB88/Trypsin (n=6)
von Frey response (% of basal)
Trypsin
Time (h)
C
Vehicle/Vehicle (n=6)
Vehicle/Trypsin (n=6)
GB88/Trypsin (n=6)
Paw withdrawl latency (s)
Trypsin
Time (h)
D
Vehicle/Vehicle (n=6)
Vehicle/Cat-S (n=6)
GB88/Cat-S (n=6)
Paw thickness (% of basal)
Cat-S
Time (h)
E
Vehicle/Vehicle (n=6)
Vehicle/Cat-S (n=6)
GB88/Cat-S (n=6)
von Frey response (% of basal)
Cat-S
Time (h)
F
Vehicle/Vehicle (n=6)
Vehicle/Cat-S (n=6)
GB88/Cat-S (6)
Paw withdrawl latency (s)
Cat-S
Time (h)
G
Vehicle / Vehicle (n=6)
Vehicle/Elastase (n=6)
GB88/Elastase (n=6)
Paw thickness (% of basal)
Elastase
Time (h)
H
Vehicle/Vehicle (n=6)
Vehicle/Elastase (n=6)
GB88/Elastase (n=6)
von Frey response (% of basal)
Elastase
Time (h)
I
Vehicle (n=5)
Elastase (n=5)
Paw withdrawl latency (s)
Elastase
Time (h)

Figure 1

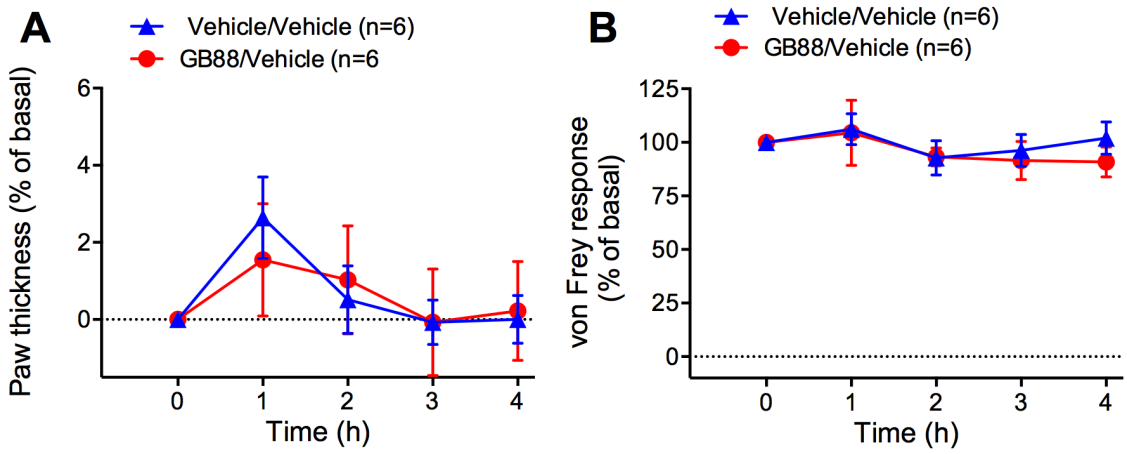
A
Vehicle/Vehicle (n=6)
GB88/Vehicle (n=6
Paw thickness (% of basal)
6
4
2
0
0
1
2
3
4
Time (h)
B
Vehicle/Vehicle (n=6)
GB88/Vehicle (n=6)
von Frey response (% of basal)
125
100
75
50
25
0
0
1
2
3
4
Time (h)

Figure 2

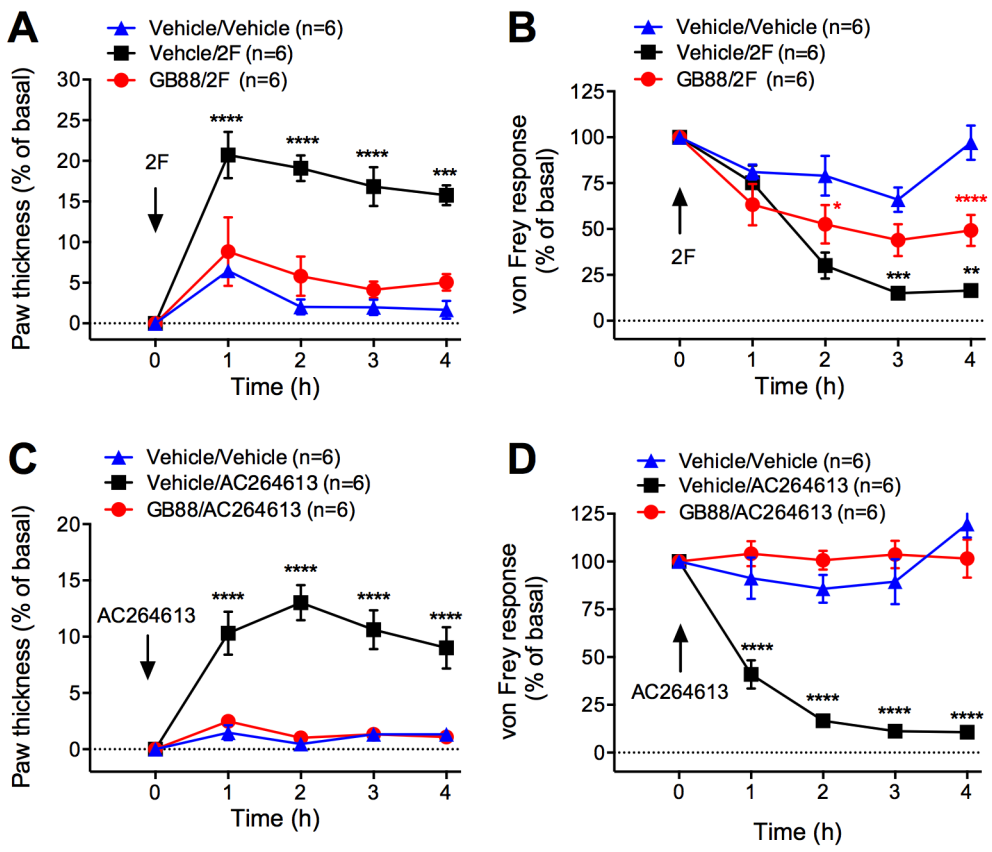
A
Vehicle/Vehicle (n=6)
Vehcle/2F (n=6)
GB88/2F (n=6)
Paw thickness (% of basal)
2F
Time (h)
B
Vehicle/Vehicle (n=6)
Vehicle/2F (n=6)
GB88/2F (n=6)
von Frey response (% of basal)
2F
Time (h)
C
Vehicle/Vehicle (n=6)
Vehicle/AC264613 (n=6)
GB88/AC264613 (n=6)
Paw thickness (% of basal)
AC264613
Time (h)
D
Vehicle/Vehicle (n=6)
Vehicle/AC264613 (n=6)
GB88/AC264613 (n=6)
von Frey response (% of basal)
AC264613
Time (h)

Figure 3

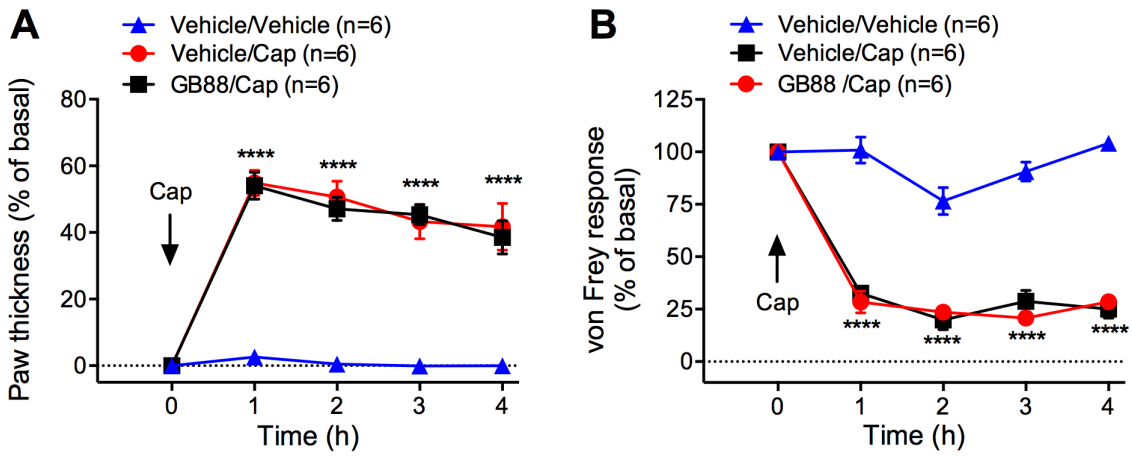
A
Vehicle/Vehicle (n=6)
Vehicle/Cap (n=6)
GB88/Cap (n=6)
Paw thickness (% of basal)
80
60
40
20
0
Cap
****
****
****
****
0
1
2
3
4
Time (h)
B
Vehicle/Vehicle (n=6)
Vehicle/Cap (n=6)
GB88 /Cap (n=6)
von Frey response (% of basal)
125
100
75
50
25
0
Cap
****
****
****
****
0
1
2
3
4
Time (h)

Figure 4

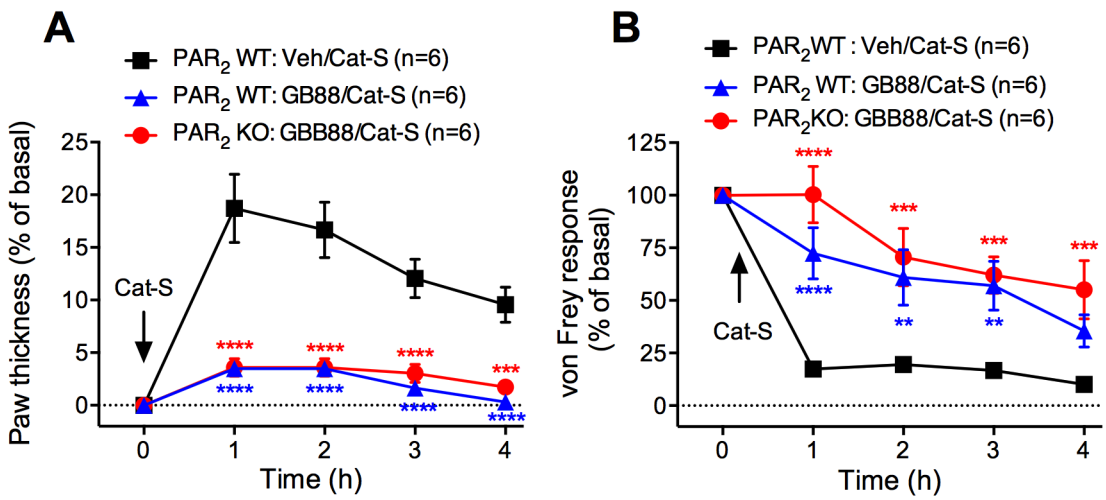
A
PAR2 WT: Veh/Cat-S (n=6)
PAR2 WT: GB88/Cat-S (n=6)
PAR2 KO: GBB88/Cat-S (n=6)
Paw thickness (% of basal)
Cat-S
Time (h)
B
PAR2WT : Veh/Cat-S (n=6)
PAR2 WT: GB88/Cat-S (n=6)
PAR2KO: GBB88/Cat-S (n=6)
von Frey response (% of basal)
Cat-S
Time (h)

Figure 5

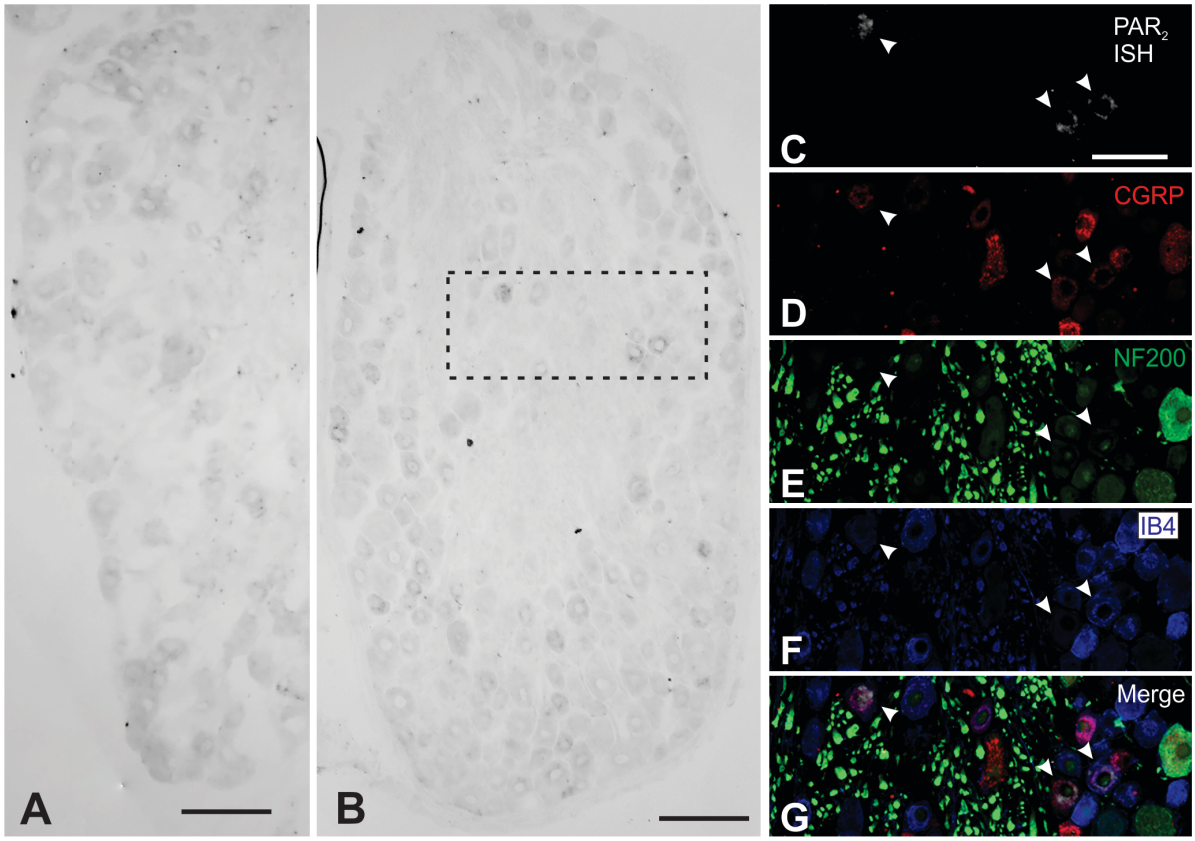

Figure 6

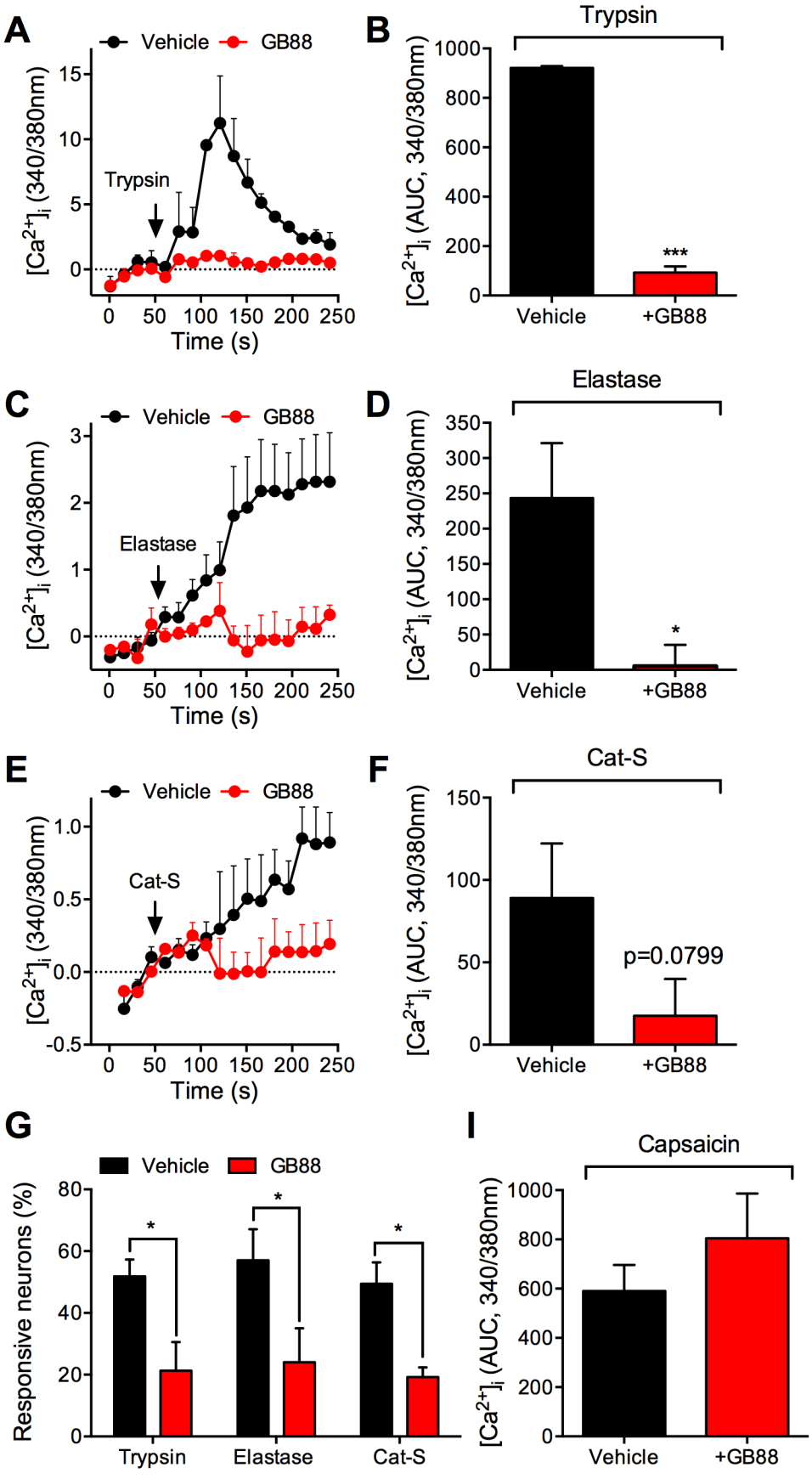
A
Vehicle
GB88
Trypsin
[Ca2+]i (340/380nm)
Time (s)
B
Trypsin
[Ca2+]i (AUC, 340/380nm)
***
Vehicle
+GB88
C
Elastase
D
Elastase
*
E
Cat-S
F
Cat-S
p=0.0799
G
Responsive neurons (%)
Trypsin
Elastase
Cat-S
I
Capsaicin

Figure 7

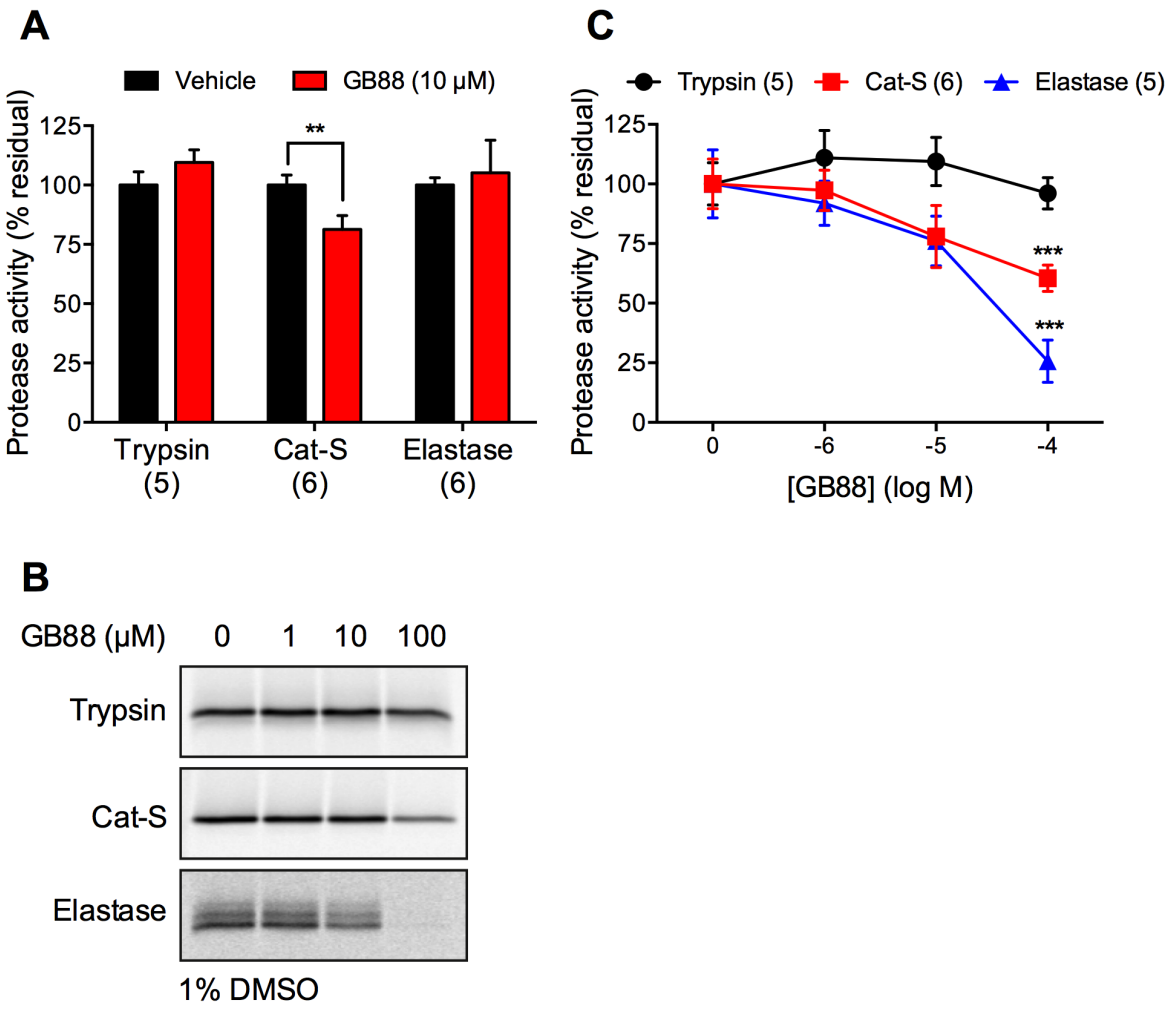
A
Vehicle
GB88 (10 μM)
Protease activity (% residual)
125
100
75
50
25
0
**
Trypsin (5)
Cat-S (6)
Elastase (6)
C
Trypsin (5)
Cat-S (6)
Elastase (5)
Protease activity (% residual)
***
***
0
-6
-5
-4
[GB88] (log M)
B
GB88 (μM)
0
1
10
100
Trypsin
Cat-S
Elastase
1% DMSO

Figure 8